

Emergence of Coherence in High Energy (Non Thermal) Plasmas Associated with Shining Black Holes

B. Coppi

Massachusetts Institute of Technology

Beijing, China June 2013

Trends Toward Ordered and Coherent Processes

- **in the Universe and in the Laboratory**

MIT Astrophysics Colloquia

Tuesday Apr 23, 2013

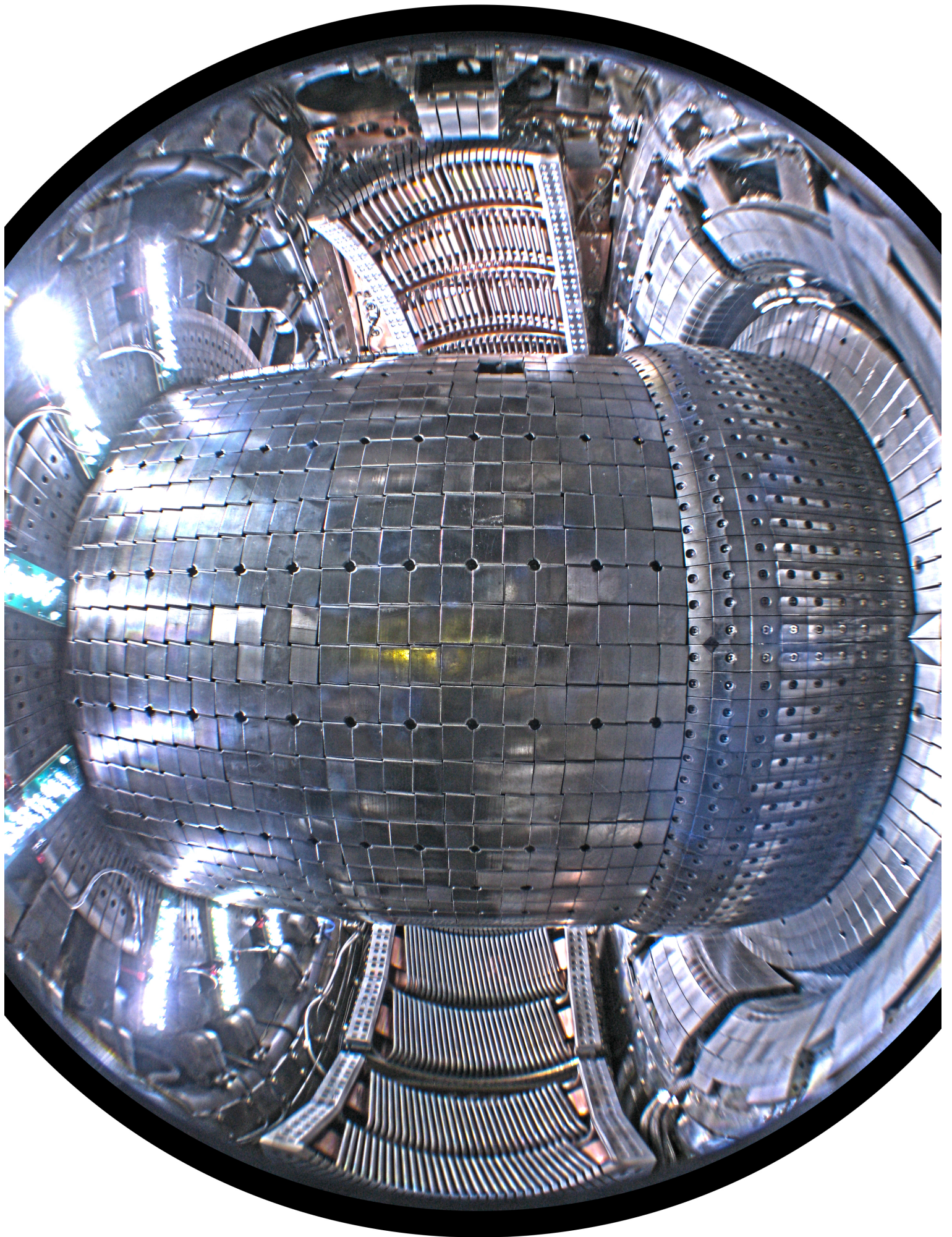
Order out of chaos: towards understanding galaxy formation in the cosmological context

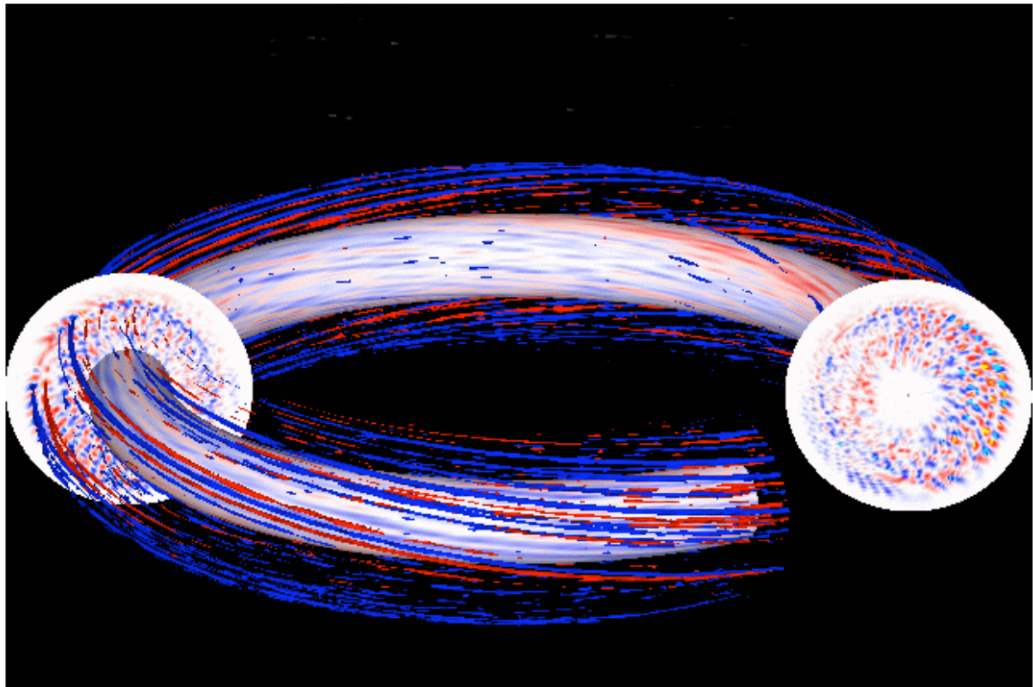
Andrey Kravtsov
U Chicago

Abstract: Galaxy formation is a complex, hierarchical, highly non-linear process, which involves gravitational collapse of dark matter and baryons, supersonic, highly compressible and turbulent flows of gas, star formation, stellar feedback, as well as heating, cooling, and chemical processes that affect the gas and, indirectly, the stellar and dark matter distributions. Nevertheless, despite the apparent complexity of processes accompanying galaxy formation, galaxies exhibit a number of striking regularities, such as tight correlations between galaxy sizes, masses, luminosities, and internal velocities and surprisingly tight correlations between properties of stars and gas in galaxies and the mass and extent of their parent halos dominated by dark matter. Existence of such correlations indicates that powerful processes operate to bring order out of chaos. Understanding what these processes are and how they operate is not only fascinating scientifically, but is critical for interpreting the avalanche of current and future observations of galaxies across cosmic time. I will describe recent progress in our understanding of how such regularities can arise in a seemingly chaotic and nonlinear process of galaxy formation.

Self Organization Processes

- **Profile Consistency in Laboratory Plasmas and in Accretion Structures (Astrophysics)**





GTC (Z. Lin, UC-Irvine)

Nonclassical Transport and the "Principle of Profile Consistency"

Starting from the experimental observation of temperature and density profiles in magnetically confined plasmas and analyzing the consistency conditions for the plasma-column equilibrium, analytical expressions for the nonclassical energy and particle flows are obtained, and an interpretation of existing experiments is provided.

The problem of understanding the nature of the particle and energy transport processes in magnetically confined plasmas has attracted considerable theoretical and experimental effort in recent years. In fact the theoretical effort has been mostly devoted to numerical simulation of the existing experimental observations, while a relatively simple analytical formulation of this problem would be highly desirable. In this spirit we present a set of criteria that appear to lead to a consistent description of both the electron thermal-energy transport and the particle transport. We label this set of criteria as the "principle of profile consistency." In fact, this is based on assuming that the observed flows of electron thermal energy and particles are those needed to reach a consistent set of radial profiles for the current density, the particle temperatures and the plasma density, while satisfying the equilibrium conditions for the considered plasma column. In addition, we start from the experimental observation that the electron temperature takes on a diffusion-like profile, in impurity-free plasmas, that is

$$T_e \simeq T_{e0} \exp\left(-\alpha_T \frac{r^2}{a^2}\right), \quad (1)$$

a being the plasma column radius and α_T a weak function of r/a . Then, to the extent that the longitudinal resistivity $\eta_{||}$ is classical, the current density profile is of the form

$$J_{||} \simeq J_0 \exp\left(-\alpha_D \frac{q_s r^2}{q_0 a^2}\right), \quad (2)$$

that is, as the combination of a diffusion process with coefficient D_p , and an inflow process^{2A} that is produced by the tendency of the density profile to settle into the diffusion profile with $\alpha_p = \alpha_T$ when the density is increased. In particular, following the trend demonstrated by a series of experiments carried out on the Alcator-A apparatus⁵ (see Figure 1), we indicate this tendency by the analytical expression

$$\alpha_p n \simeq \alpha_T n_0 \frac{n + n_0^0}{n_0 + 2\alpha_T n_0^0 (1-r^2/a^2)^{1/2}} \quad (14)$$

Note that when $n_0 < \alpha_T n_0^0$ the density profile is wider than and decoupled from the electron temperature profile. A clear experimental indication of this is in fact shown by Figure 2. On the other hand, as the density is decreased while sufficiently high electron temperature is maintained, the particle inflow Γ_w due to the so-called Ware drift associated with the presence of trapped electrons should be considered.⁶ Then the central density profile can be derived from the equation

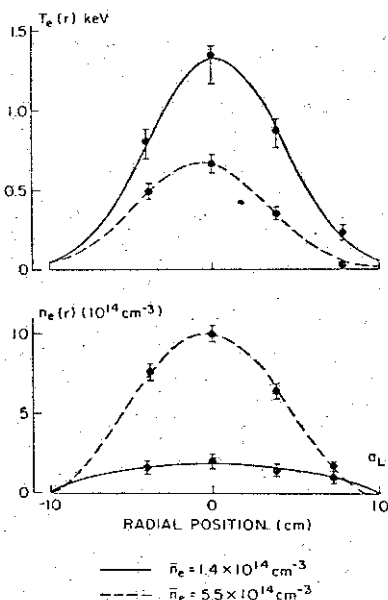
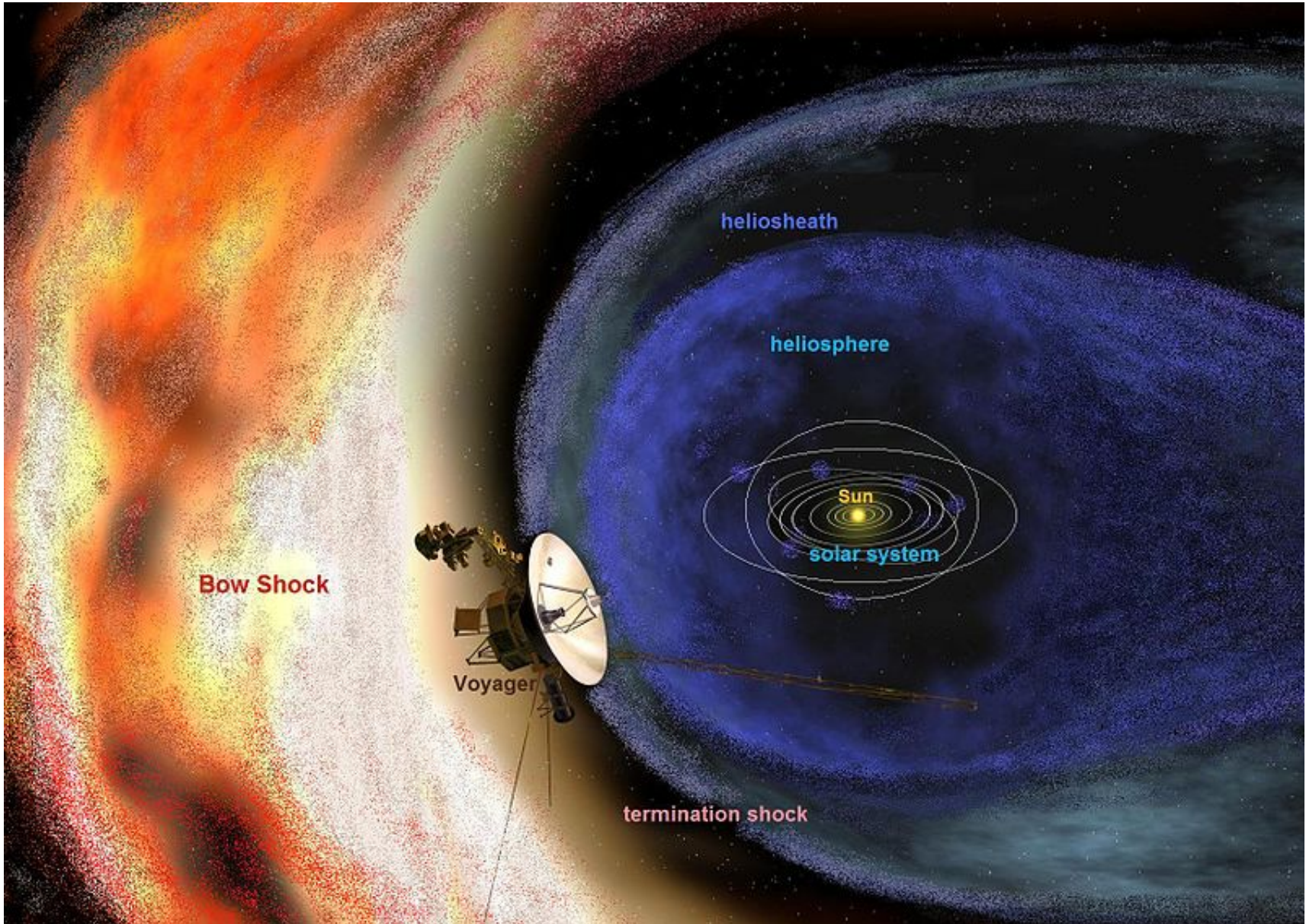


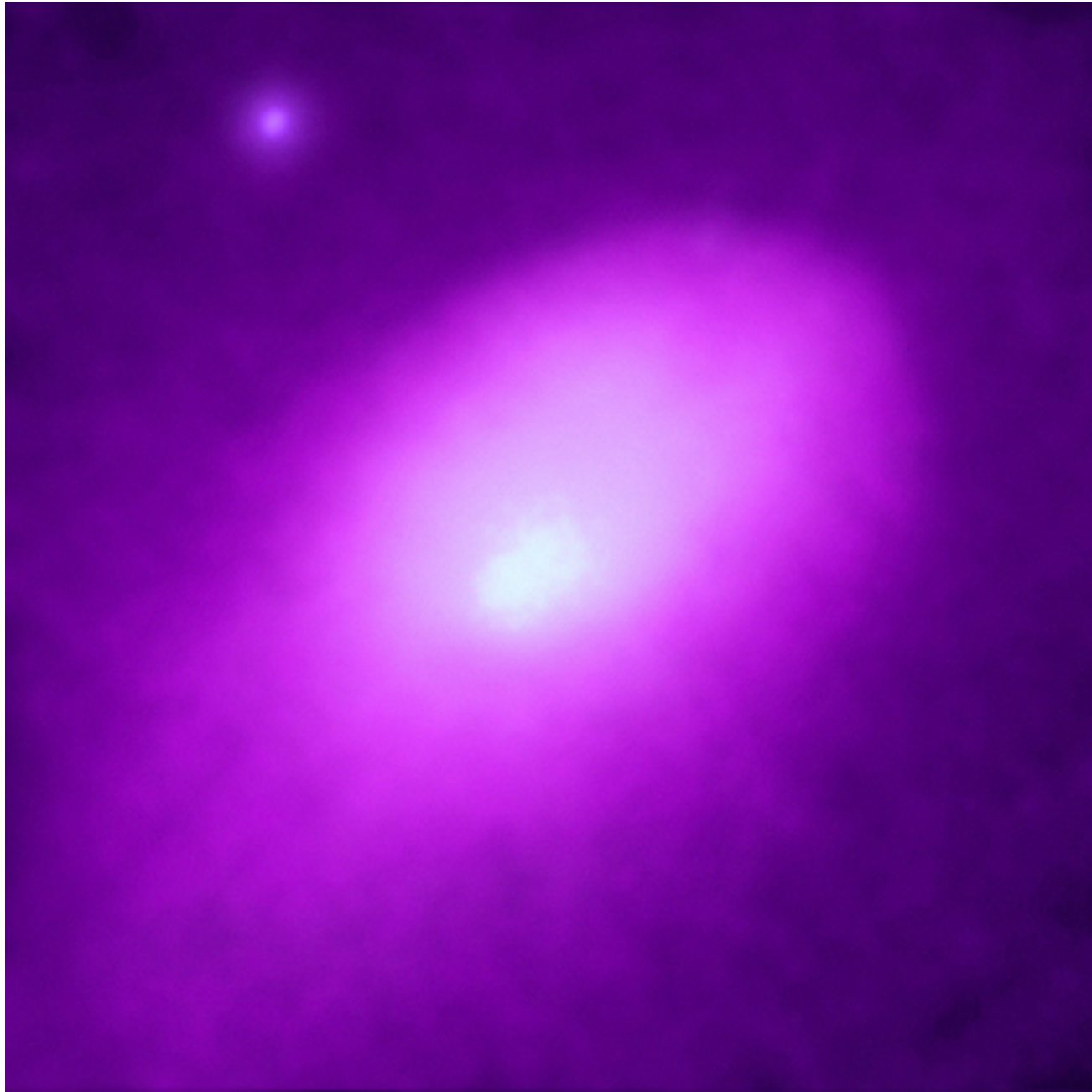
FIGURE 1. Radial profiles of electron temperature and density at two different values of the linear average density \bar{n}_e , for deuterium plasmas obtained in the Alcator-A device.⁵ The relevant value of the toroidal field is $B_T = 60$ kG, and the plasma current is in the range $130 \text{ kA} \leq I \leq 160 \text{ kA}$. The major radius $R = 54$ cm, the minor radius $a = 10$ cm and the resistive loop voltage $V \simeq 2.4$ V.



Based on NASA Free File Courtesy NASA/JPL-Caltech.



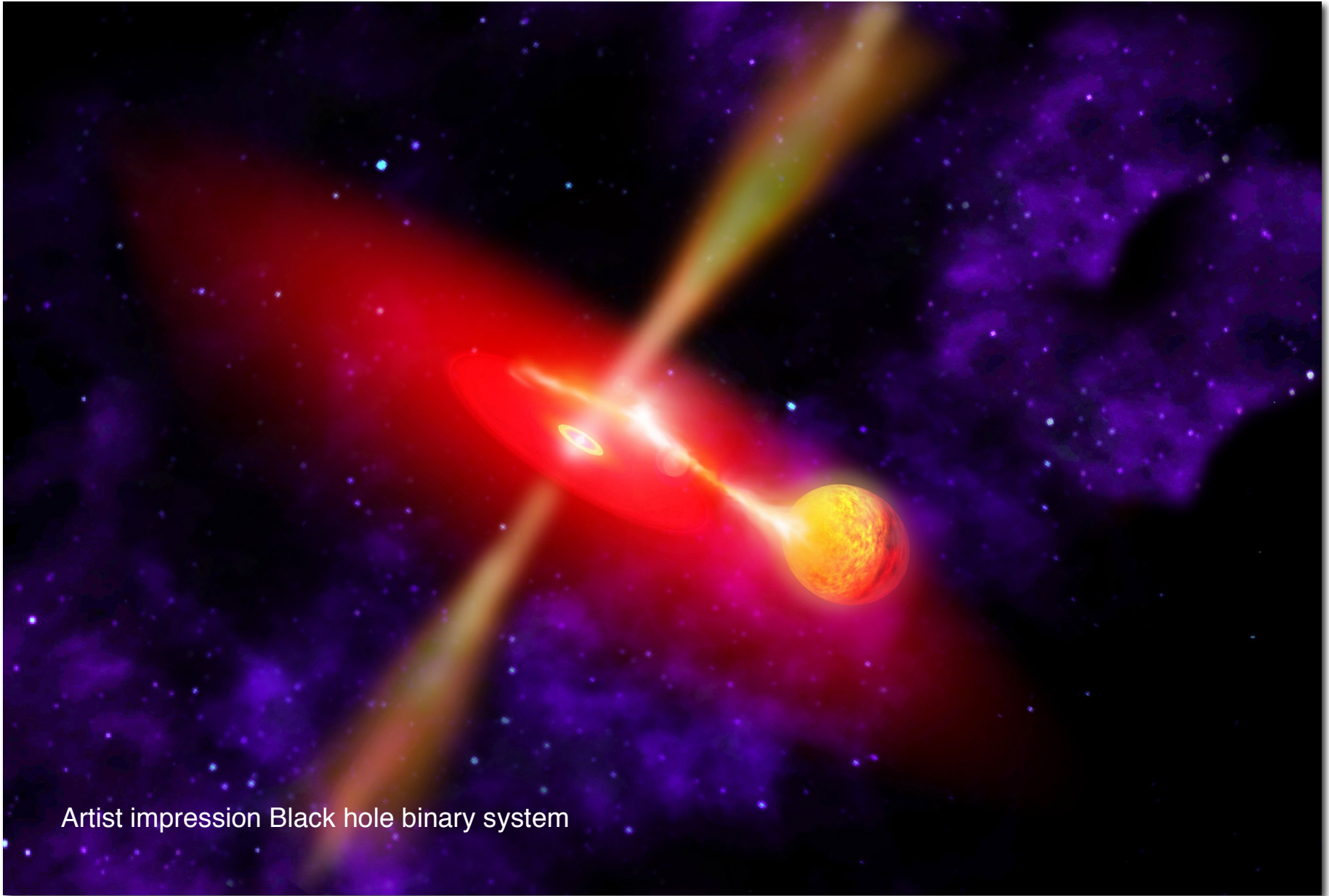
The massive galaxy cluster Abell 1689, with member galaxies shown in white along with the hot X-ray emitting gas in blue. Credit: X-ray: NASA/CXC/MIT/E.-H Peng. Optical: NASA/STScI



UCLA astronomer George Ogden Abell

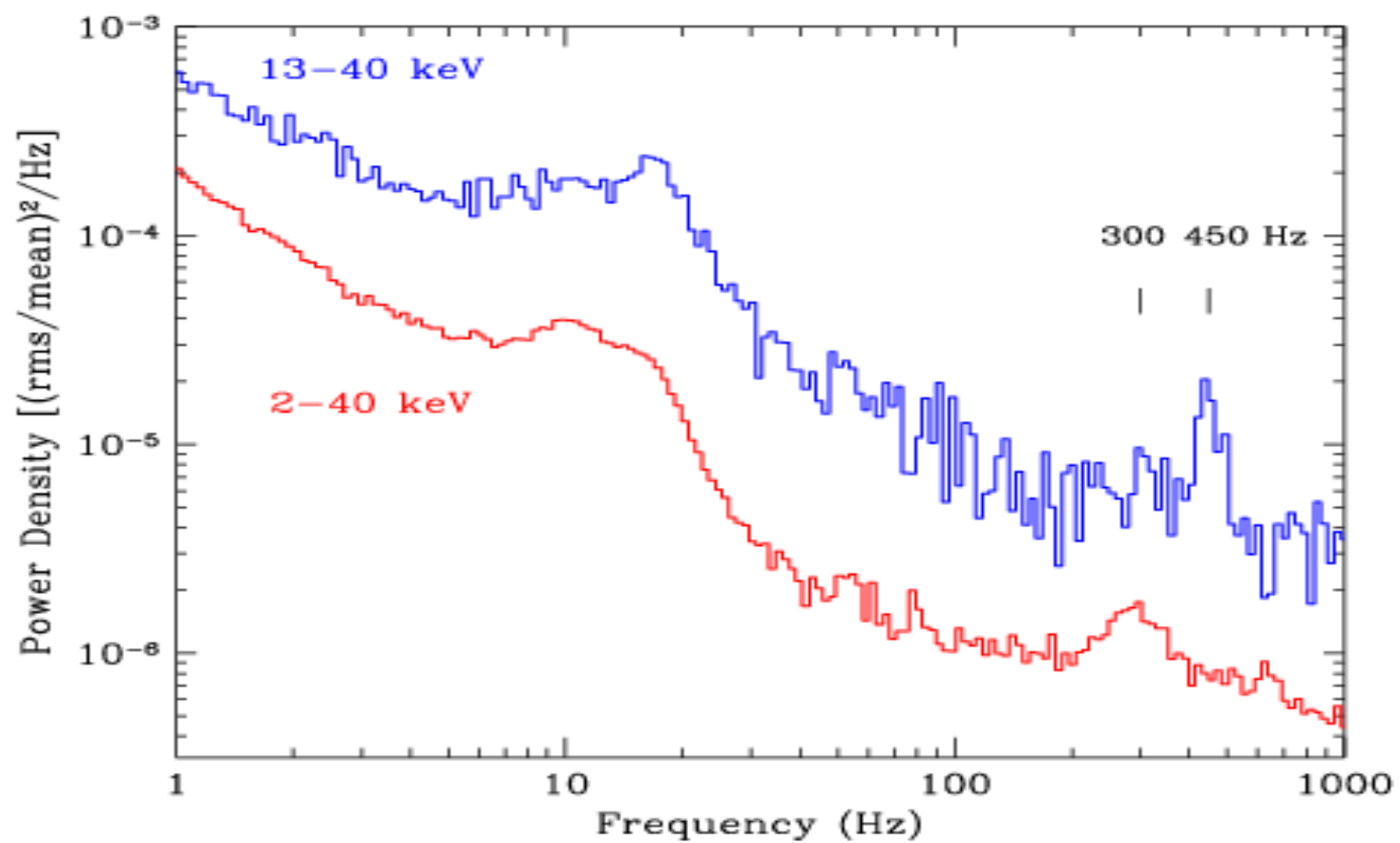
Chandra X-ray Observatory image of the galaxy cluster Abell 2142. The image shows a colossal cosmic "weather system" produced by the collision of two giant clusters of galaxies. For the first time, the pressure fronts in the system can be traced in detail, and they show a bright, but relatively cool 50 million degree central region (white) embedded in large elongated cloud of 70 million degree gas (magenta), all of which is roiling in a faint atmosphere of 100 million degree gas (faint magenta and dark blue). The bright source in the upper left is an active galaxy in the cluster.

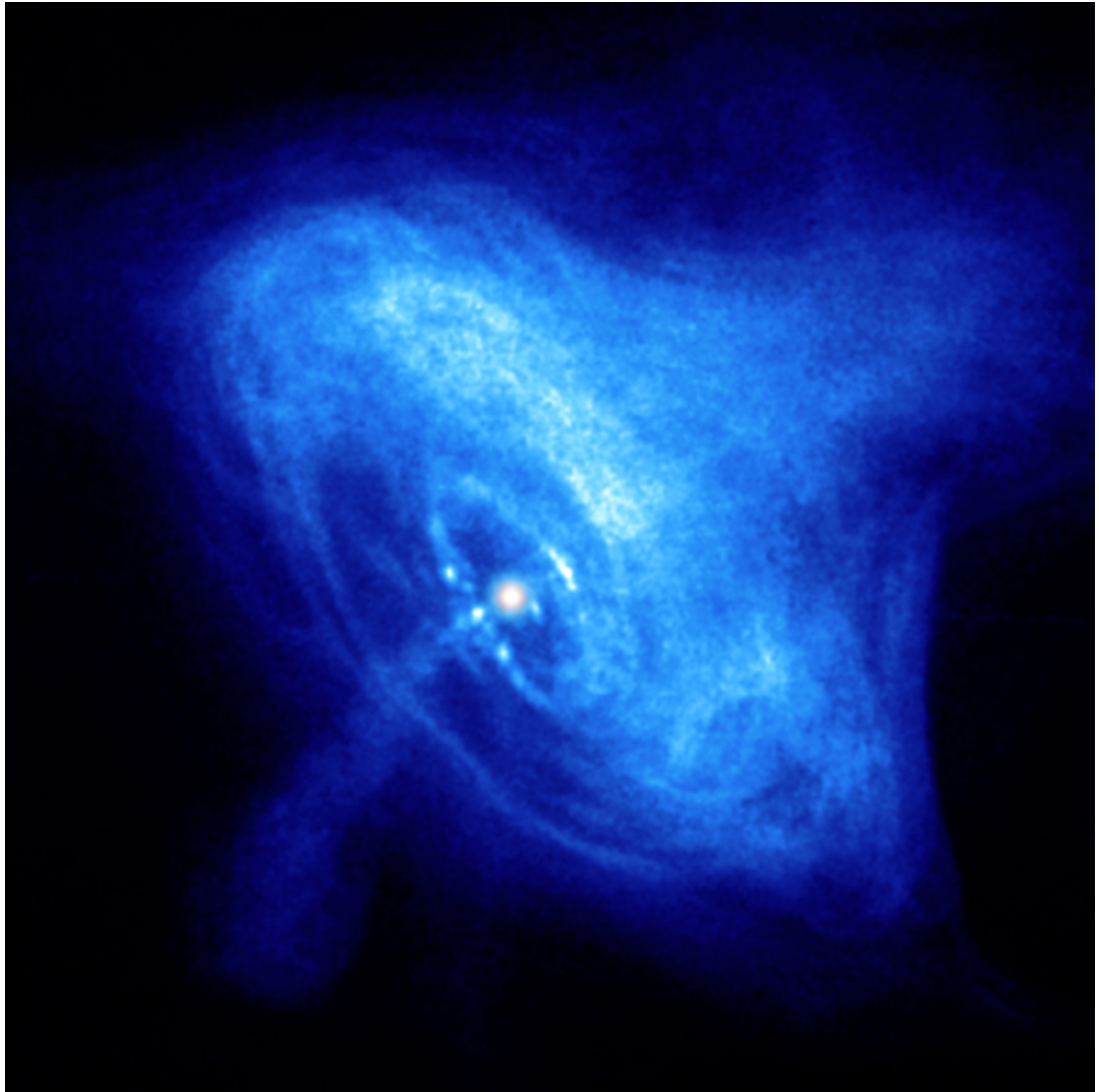
Abell 2142 is six million light years across and contains hundreds of galaxies and enough gas to make a thousand more. It is one of the most massive objects in the universe. Galaxy clusters grow to vast sizes as smaller clusters are pulled inward under the influence of gravity. They collide and merge over the course of billions of years, releasing tremendous amounts of energy that heats the cluster gas. The smoothness of the elongated cloud in the Chandra image suggests that these sub-clusters have collided two or three times in a billion years or more, and have nearly completed their merger.

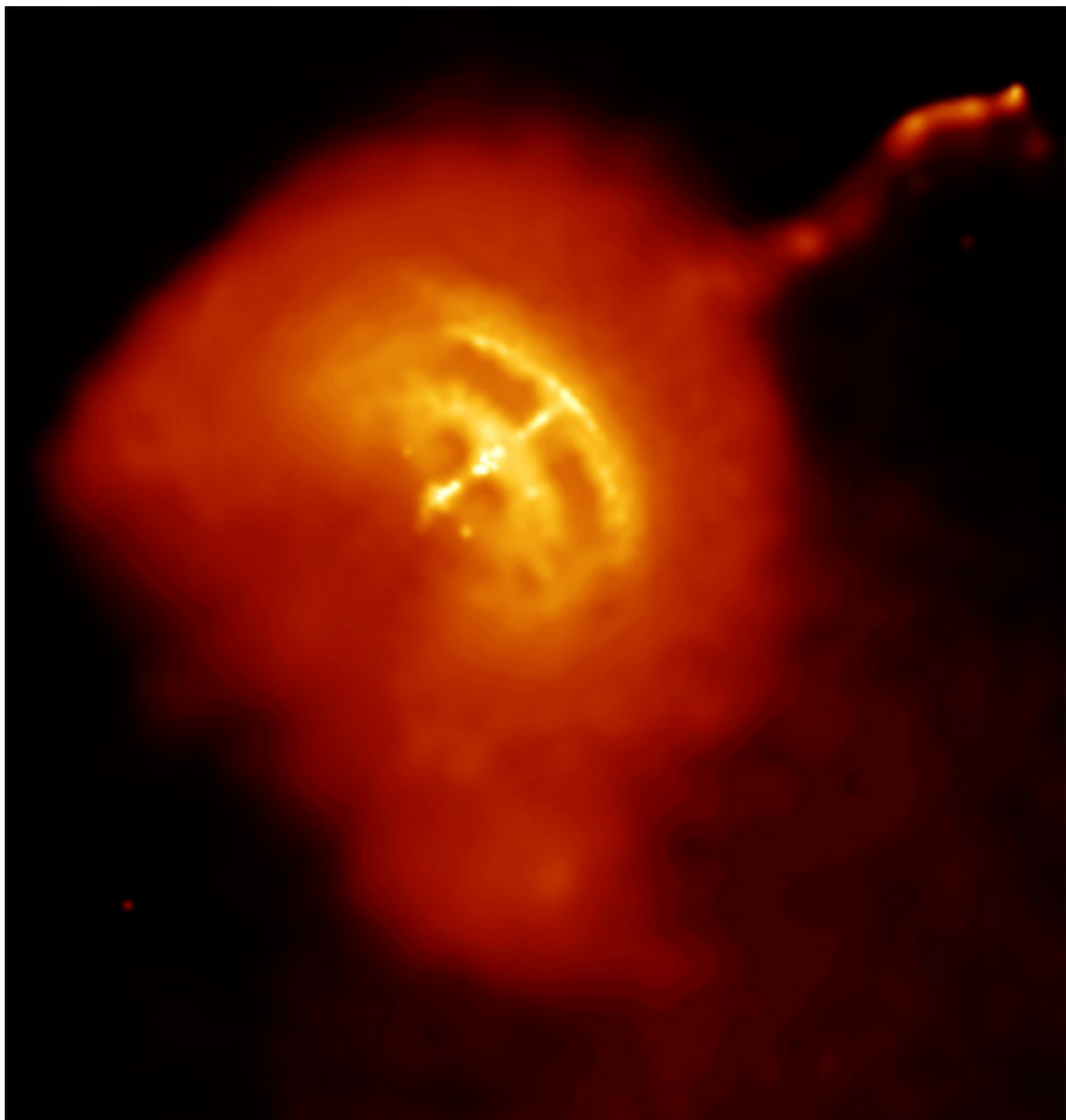


Artist impression Black hole binary system

Black Hole Binary, GROJ1655-40 in 1996 outburst
selected observations in the Steep Power Law State







The radiation emission from Shining Black Holes is most frequently observed to have non thermal features. Therefore, it is appropriate to consider relevant collective processes of plasmas surrounding black holes and containing high energy particles with non-thermal distributions in momentum space. The main subjects that are dealt with are: a) the existence and characteristics of stationary plasma and field configurations; b) the excitation of magneto-gravitational modes driven by temperature anisotropies and differential rotation; c) the generation of magnetic fields over macroscopic scale distances.

2. Sustaining Factors

The sustaining factor of new characteristic field configurations that can emerge in plasmas in the immediate surroundings of black holes can be identified by applying the $\mathbf{e}_\phi \cdot \nabla \times$ operator to the total momentum conservation equation

$$\rho (\nabla \Phi_G - \Omega^2 R \mathbf{e}_R) = -\nabla \cdot \mathbb{P} + \frac{1}{c} \mathbf{J} \times \mathbf{B}. \quad (2.1)$$

Here we refer to an axisymmetric plasma configuration, we assume that only a rotation velocity ΩR is present, R is the distance from the axis of symmetry, Φ_G is the gravitational potential and \mathbb{P} is the relevant pressure tensor. Then we consider

$$\mathbb{P} = p\mathbb{I} + \Delta\mathbb{P}, \quad (2.2)$$

where the non isotropic component $\Delta\mathbb{P}$ is significant, and we identify the sustaining factor for the relevant magnetic field configuration as

$$D \equiv \mathbf{e}_\phi \cdot \nabla \times \left[\nabla \cdot (\Delta\mathbb{P}) + \rho (\nabla \Phi_G - \Omega^2 R \mathbf{e}_R) \right]$$

in which $\mathbf{A}_N \equiv \nabla \cdot (\Delta\mathbb{P})$ adds its influence to that of the gravitational field and rotation. In particular

$$D \simeq \frac{\partial}{\partial z} A_{NR} - \frac{\partial}{\partial R} A_{Nz} - \left(\frac{\partial \rho}{\partial z} \right) \left[R\Omega^2 - \frac{\partial \Phi_G}{\partial R} \right] - R\rho \frac{\partial}{\partial z} \Omega^2 - \frac{\partial \Phi_G}{\partial z} \frac{\partial \rho}{\partial R} \quad (2.3)$$

where $R^2\Omega^2 \simeq \partial\Phi_G/\partial R$ and we consider

$$D_{AN} \equiv \left| \mathbf{e}_\phi \cdot \nabla \times [\nabla \cdot (\Delta\mathbb{P})] \right| \sim \left| \frac{\partial \Phi_G}{\partial z} \frac{\partial \rho}{\partial R} \right|. \quad (2.4)$$

The simplest way to avoid having to deal with phase space and to maintain a fluid description is to refer to plasmas with particle populations that can be described by bi-Maxwellian distributions in momentum space with two temperatures T_{\parallel} and T_{\perp} . In particular we take T_{\parallel} to be the prevalent temperature in a given direction and we assume that the plasma is composed of two populations: a thermal population with an isotropic plasma pressure $p = 2nT$, n being the electron density, and a super thermal population with $p_{\parallel} > p$ and $T_{\parallel} > T$.

2. Rigidly Rotating Rings Associated with Non-Thermal Distributions in Momentum Space

We consider a radial interval around $R - R_0$ within which the rotation frequency $\Omega(R) \simeq \Omega_0$ in the sense that $|(R/\Omega) d\Omega/dR| \ll 1$. Referring to plasmas with two particle populations as indicated earlier.

$$\mathbb{P} = p\mathbb{I} + (p_{\parallel} - p) \mathbf{e}_{\parallel}\mathbf{e}_{\parallel}. \quad (2.1)$$

An important special case to analyze is that for which the pressure anisotropy is connected with the direction of the magnetic field. Thus

$$\Delta\mathbb{P} = (p_{\parallel} - p) \frac{\mathbf{B}\mathbf{B}}{B^2}. \quad (2.2)$$

Another case is that for which the anisotropy is connected with the direction of the rotation velocity, that is $\Delta\mathbb{P} = (p_{\parallel} - p) \mathbf{e}_{\phi}\mathbf{e}_{\phi}$. In this case if we consider an axisymmetric configuration we have

$$\nabla \cdot (\Delta\mathbb{P}) = -(p_{\parallel} - p) \frac{1}{R} \mathbf{e}_{\phi}. \quad (2.3)$$

In the former case, referring to axisymmetric configurations and defining

$$\bar{p} = \frac{4\pi}{B^2} (p_{\parallel} - p) \quad (2.4)$$

we find that

$$\nabla \cdot (\Delta\mathbb{P}) = \frac{1}{4\pi} \mathbf{B} \cdot \nabla (\bar{p}\mathbf{B}). \quad (2.5)$$

Therefore

$$\begin{aligned} -\nabla \cdot \mathbb{P} + \frac{1}{c} \mathbf{J} \times \mathbf{B} = \\ -\nabla \left(p + \frac{B^2}{8\pi} \right) + \frac{1}{4\pi} \mathbf{B} \cdot [(1 - \bar{p}) \mathbf{B}] \end{aligned} \quad (2.6)$$

where \mathbf{B} is represented by

$$\mathbf{B} = \frac{1}{R} \left[\nabla\psi \times \mathbf{e}_{\phi} + I(\psi, z) \mathbf{e}_{\phi} \right] \quad (2.7)$$

and $\psi(R, z)$ is the familiar magnetic surface function as $\mathbf{B} \cdot \nabla\psi = 0$

In this case the Master Equation that we use, together with the vertical component of Eq. (1.1), to identify stationary plasma and field configurations is

$$\begin{aligned} \mathbf{e}_{\phi} \cdot \{ \nabla\rho \times \nabla\Phi_G - \nabla \times (\rho\Omega R\mathbf{e}_R) \} \\ \simeq \frac{1}{4\pi} \mathbf{e}_{\phi} \cdot \{ \nabla \times [\mathbf{B} \cdot \nabla ((1 - \bar{p}) \mathbf{B})] \}. \end{aligned} \quad (2.8)$$

Then, for radially localized configurations, we consider a special class of solutions for which ψ can be represented by

4. Examples of Anisotropy Driven Configurations

We consider radially localized configurations around $R = R_0$. In this case the l.h.s. of the Master Equation (2.8) becomes simply

$$-\Omega^2_0 \left[z \frac{\partial \rho}{\partial R} + 3 (R - R_0) \frac{\partial \rho}{\partial z} \right], \quad (4.1)$$

where $\Omega_0 \equiv \Omega_k (R = R_0)$, while the r.h.s. is

$$\frac{1}{4\pi} \left\{ \frac{\partial}{\partial z} [\mathbf{B} \cdot \nabla ((1 - \bar{p}) B_R)] - \frac{\partial}{\partial R} [\mathbf{B} \cdot \nabla ((1 - \bar{p}) B_z)] \right\}. \quad (4.2)$$

Then we look for configurations such that

$$\psi = \psi_N \psi_*(R_*) \exp\left(-\frac{\bar{z}^2}{2}\right) \quad (4.3)$$

where $R_* \equiv (R - R_0)/\Delta_R$, $\bar{z} \equiv z/\Delta_z$, $\Delta_R^2 < \Delta_z^2 \ll R_0^2$ and $\psi_*(R_*) \sim 1$, and, correspondingly $\rho = \rho_N \rho_*(R_*) \exp(-\bar{z}^2)$ where $\rho_*(R_*) \sim 1$.

In this case the Master Equation reduces to

$$\begin{aligned} & \Omega^2_0 \left[\frac{\partial \rho}{\partial R} - \frac{6}{\Delta_z^2} (R - R_0) \rho \right] z \\ & \simeq -\frac{1}{4\pi} \frac{\partial}{\partial R} \left\{ B_R \frac{\partial}{\partial R} [(\bar{p} - 1) B_z] + B_z \frac{\partial}{\partial R} [(\bar{p} - 1) B_z] \right\}. \end{aligned} \quad (4.4)$$

Equation (3.4) can be viewed as an inhomogeneous equation whose solution is of the form

$$\rho = \Delta\rho + \rho^h \quad (4.5)$$

where

$$\frac{\partial \rho^h}{\partial R_*} - \left(\frac{6\Delta_R^2}{\Delta_z^2} \right) R_* \rho^h = 0 \quad (4.6)$$

that is

$$\rho^h = \rho_0^h \exp \left[- \left(\frac{3\Delta_R^2}{\Delta_z^2} \right) R_*^2 \right] \quad (4.7)$$

while

$$\frac{\partial}{\partial R_*} \Delta\rho + \left(\frac{6\Delta_R^2}{\Delta_z^2} \right) R_* \Delta\rho \simeq - \frac{1}{4\pi\Omega_0^2 z} \frac{\partial}{\partial R_*} \left\{ B_R \frac{\partial}{\partial R} [(\bar{p} - 1) B_z] + B_z \frac{\partial}{\partial R} [(\bar{p} - 1) B_z] \right\}. \quad (4.8)$$

The vertical momentum conservation equation to be combined with the Master Equation in order to find compatible solutions for ρ , ψ and p , is

$$z\Omega_0^2 \rho \simeq - \frac{\partial}{\partial z} \left(p + \frac{B^2}{8\pi} \right) + \frac{1}{4\pi} \left(\mathbf{B} \cdot \nabla [(1 - \bar{p}) \mathbf{B}] \right)_z. \quad (4.9)$$

This can be rewritten as

$$\rho \simeq - \frac{1}{\Omega_0^2 z} \frac{\partial}{\partial z} \left(p + \frac{B^2}{8\pi} \right) - \frac{1}{4\pi\Omega_0^2 z} \left\{ B_R \frac{\partial}{\partial R} [(\bar{p} - 1) B_z] + B_z \frac{\partial}{\partial R} [(\bar{p} - 1) B_z] \right\}. \quad (4.10)$$

Then we can find a solution with

$$\Delta\rho \simeq - \frac{1}{4\pi\Omega_0^2 z} \left\{ (\bar{p} - 1) \left(B_R \frac{\partial}{\partial R} B_z + B_z \frac{\partial}{\partial z} B_z \right) + B_z \left(B_R \frac{\partial}{\partial R} \bar{p} + B_z \frac{\partial}{\partial z} \bar{p} \right) \right\} \quad (4.11)$$

and

$$\frac{\partial}{\partial z} \left(p + \frac{B^2}{8\pi} \right) = -\Omega_0^2 z \rho^h \quad (4.12)$$

that is

$$p \simeq \frac{1}{2} \Omega_0^2 \Delta_z^2 \rho^h - \frac{B^2}{8\pi}. \quad (4.13)$$

Clearly, the expression (3.11) for $\Delta\rho$ is the same as the approximate solution of Eq. (3.8).

At this point we may assume, for the sake of simplicity, that $\bar{p} \approx \bar{p}_0 \exp[-(3\Delta_R^2 R_*^2/\Delta_z^2)]$. Thus

$$\Delta\rho \approx \frac{(\bar{p}_0 - 1)}{4\pi\Omega_0^2\Delta_z^2 R_0^2} \left\{ \left(\frac{\partial\psi}{\partial R} \right)^2 - \psi \frac{d^2\psi}{dR^2} \right\} \quad (4.14)$$

and if we take

$$\psi_* \approx (\sin R_*) \exp\left(-\frac{\sigma}{2} R_*^2\right) \quad (4.15)$$

we obtain

$$\Delta\rho \approx \frac{(\bar{p}_0 - 1) B_N^2}{4\pi\Omega_0^2\Delta_z^2} \exp(-\sigma R_*^2 - \bar{z}^2) [1 + \sigma \sin^2 R_*] \quad (4.16)$$

where

$$3\frac{\Delta_R^2}{\Delta_z^2} < \sigma < 1. \quad (4.17)$$

It is evident that Eq. (3.16) represents a ring configuration that emerges when $p_1 > p + B^2/(4\pi)$.

We notice that no seed magnetic field needs to be introduced in order to find plasma and field configurations of the type we have considered. Thus we may argue that the emergence of these configurations is the result of collective modes which greatly amplify magnetic fields until the magnetic pressure becomes of the order of the gravitationally confined plasma pressure.

Solitary Ring Solution (cont.)

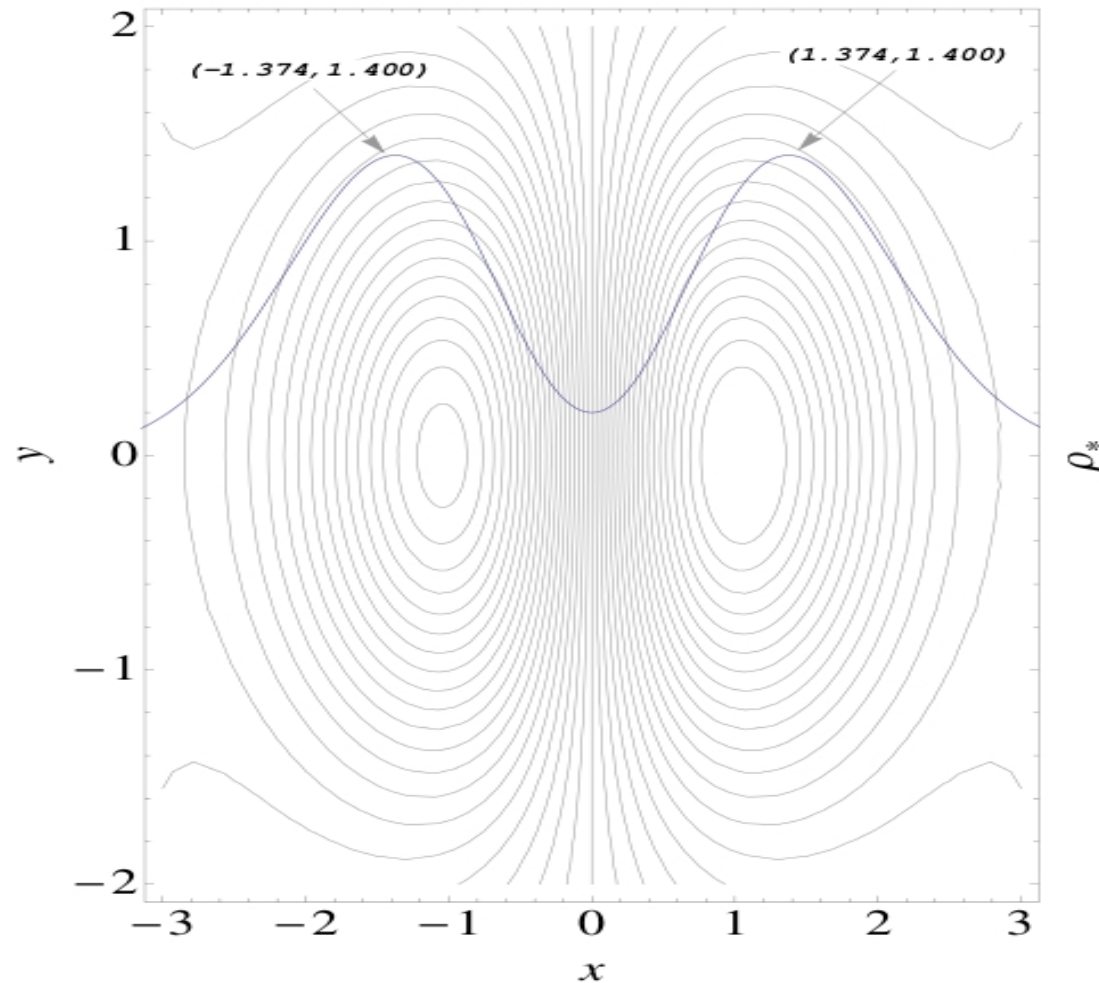


Figure: Graphical representation of the magnetic surfaces for the configuration corresponding to Eq. (38). The curve with dotted heavy lines indicates the single ring density profiles represented by Eq. (39) for $\Delta_R^2/\Delta_z^2 = 1/10$.

4. Plasma Collective Modes

An issue to be dealt with is whether the presence of high energy particle populations with non-Maxwellian distributions can have a significant influence on the modes that can be excited in plasma disks surrounding black holes. The interest in these modes, identified as Magneto-Gravitational Modes as they depend on both gravity and the related differential rotation, is that they lead to a strong amplification of the seed magnetic field in which the original unperturbed disks are imbedded, and produce ring structures of the kind that can be found as non linear solutions of the equations for stationary plasma and field configurations surrounding a black hole. Another important feature of these modes is that they can transport angular momentum in the outward direction and, as is well known, this is a necessary process for the occurrence of accretion onto the central black hole.

The tri-dimensional geometry of the rings that are shown to emerge from an axisymmetric disk and that involve rotating and trailing density spirals lend themselves to be a well founded candidate for the so-called Quasi Periodic Oscillations of the X-ray emission from galactic black holes.

6. Currentless Disk and Relevant Perturbations

The plasma configuration that is considered for the excitation of the most elementary modes is the classical axisymmetric disk imbedded in a seed vertical magnetic field and in which no current is present. The only flow velocity present is the Keplerian rotation around the axis of symmetry. The vertical equilibrium condition, is for $\mathbf{B} = B\mathbf{e}_z$ with $B = \text{const}$ over the height of the disk,

$$\Omega_k^2 \rho z = -\frac{\partial p_1}{\partial z}. \quad (6.1)$$

The rotation frequency is about constant over the height of the disk and given by

$$\Omega_k = \left(\frac{GM_*}{R^3} \right)^{1/2} \quad (6.2)$$

where M_* is the mass of the black hole in the center of the disk as we refer to radial distances $R \gg H$, where

$$H^2 \sim \frac{p_1}{\rho \Omega_k^2}. \quad (6.3)$$

We consider perturbations of the toroidal velocity $\Omega_0 R$ of the form

$$\hat{v}_\phi = \tilde{v}_\phi(R - R_0, z) \exp \{ \gamma_0 t - im_\phi (\Omega_0 t - \phi) \} \quad (6.4)$$

where

$$\tilde{v}_\phi(R - R_0, z) \simeq \tilde{v}_\phi(z) F(R - R_0) \exp [ik_R (R - R_0)], \quad (6.5)$$

$F(R - R_0)$ is a localized function around $(R = R_0)$ over a distance of the order of Δ_R , with $1/k_R^2 \ll \Delta_R^2 \ll R_0^2$ and $\Omega \equiv \Omega_k(R - R_0)$. Thus

$$\frac{d}{dt} \hat{v}_\phi = \gamma_0 + im_\phi [\Omega_k(R) - \Omega_0] \simeq \gamma_0 + im_\phi (d\Omega_k/dR) (R - R_0) \quad (6.6)$$

and

$$\hat{v}_\phi \simeq \tilde{v}_\phi(z) F(R - R_0) \exp \{ \gamma_0 t + i(R - R_0) [k_R + m_\phi (d\Omega_k/dR)t] - im_\phi [\Omega_k(R)t - \phi] \}. \quad (6.7)$$

At first we shall analyze axisymmetric perturbations for which $m_\phi = 0$ and $dF/dR \simeq 0$

7. Linearized Perturbed Equations

We consider modes that are localized vertically around $z=0$. Thus we may refer to a generic unperturbed density profile

$$\rho \simeq \rho_0 \left(1 - \frac{z^2}{H_0^2} \right). \quad (7.1)$$

The perturbed mass conservation equation is

$$\hat{\rho} - \frac{2z}{H_0^2} \rho_0 \hat{\xi}_z + \rho_0 \nabla \cdot \hat{\xi} \simeq 0 \quad (7.2)$$

where $\hat{v}_z = \gamma_0 \hat{\xi}_z$, is the vertical velocity and

$$\nabla \cdot \hat{\xi} \simeq ik_R \hat{\xi}_R + \frac{\partial \hat{\xi}_z}{\partial z}. \quad (7.3)$$

In particular we choose to consider

$$|\nabla \cdot \hat{\xi}| \lesssim \left| \frac{z}{H_0^2} \hat{\xi}_z \right| \quad (7.4)$$

such as $\nabla \cdot \hat{\xi} = 0$ for “incompressible” modes. Moreover, referring to the analysis carried out in the absence of pressure anisotropy [Coppi, 2012] and to modes for which $z\Omega_k^2 \hat{\rho} \sim \partial \hat{p} / \partial z$ we note that

$$\frac{\hat{p}}{\rho} \sim z^2 \Omega_k^2 \frac{\hat{\rho}}{\rho} \sim \frac{\hat{\rho}}{\rho} \frac{z^2}{H_0^2}. \quad (7.5)$$

Therefore for $z^2 \sim \Delta_z^2 \ll H_0^2$, $|\hat{p}/\rho| \ll |\hat{v}/\rho|$, and taking

$$\gamma_0 \hat{p} + \frac{dp}{dz} \hat{\xi}_z + \Gamma_p \rho \nabla \cdot \hat{\xi} = 0 \quad (7.6)$$

we find

$$\nabla \cdot \hat{\xi} \simeq -\frac{1}{\Gamma_p} \frac{dp}{dz} \frac{1}{\rho} \hat{\xi}_z \quad (7.7)$$

where $p = 2nT$, $n = \rho/m_i$ and $1/\Delta_z^2 \sim |\partial^2 \hat{\xi}_z / \partial z^2| / |\hat{\xi}_z|$. In this case if we define

$$\eta_T \equiv \frac{1}{T} \frac{dT}{dz} / \frac{1}{n} \frac{dn}{dz} \quad (7.8)$$

we find

$$\frac{\hat{p}}{\rho_0} \simeq -\frac{2z}{H_0^2} \hat{\xi}_z \left(\frac{\Gamma_p - 1}{\Gamma_p} - \frac{1}{\Gamma_p} \eta_T \right) \equiv \frac{2z}{H_0^2} \hat{\xi}_z D_N. \quad (7.9)$$

Next we refer to the toroidal momentum conservation equation that is

$$\begin{aligned} & \rho_0 \left[\frac{\partial \hat{v}_\phi}{\partial t} + (\hat{v} \cdot \nabla \mathbf{v} + \mathbf{v} \cdot \nabla \hat{v})_\phi \right] \\ & \simeq \frac{1}{4\pi} [\mathbf{B} \cdot \nabla (1 - \bar{\rho}) \hat{\mathbf{B}}]_\phi. \end{aligned} \quad (7.10)$$

Then

$$\rho_0 \left(\gamma_0 \hat{v}_\phi + \gamma_0 \hat{\xi}_R R \frac{d\Omega_k}{dR} + 2\Omega_k \gamma_0 \hat{\xi}_R \right) \simeq \frac{1}{4\pi} B_z (1 - \bar{\rho}) \frac{\partial}{\partial z} \hat{B}_\phi \quad (7.11)$$

and, if

$$\psi_\phi = -\frac{d\Omega}{dR} R \hat{\xi}_R + \gamma_0 \hat{\xi}_\phi \quad (7.12)$$

$$\hat{B}_\phi = B \frac{\partial \hat{\xi}_\phi}{\partial z} \quad (7.13)$$

as we shall justify, we obtain

$$(1 - \bar{p}) v_A^2 \frac{\partial^2}{\partial z^2} \hat{\xi}_\phi = \gamma_0^2 \hat{\xi}_\phi + 2\gamma_0 \Omega k \hat{\xi}_R \quad (7.14)$$

where $v_A^2 \equiv B^2 / (4\pi\rho_0)$.

Therefore, if we define

$$c_{\parallel}^2 \equiv \frac{P_1 - P}{\rho} \quad (7.20)$$

we have

$$\hat{\xi}_{\phi k} \simeq 2\Omega_0 \gamma_0 \frac{\kappa}{k_R} \frac{\hat{\xi}_{zk}}{\gamma_0^2 + \kappa^2 (v_A^2 - c_{\parallel}^2)}. \quad (7.21)$$

Finally, the so called Frozen-in-Law is represented by the equation

$$\gamma_0 \hat{\mathbf{B}} = \nabla \times (\hat{\psi} \times B \mathbf{e}_z + R \Omega \mathbf{e}_\phi \times \hat{\mathbf{B}}). \quad (7.22)$$

This gives

$$\gamma_0 \hat{B}_\phi = B \frac{\partial}{\partial z} \psi_\phi + \hat{B}_R \frac{d}{dR} (R\Omega) - R\Omega \frac{\hat{B}_R}{R} = B \frac{\partial}{\partial z} \left(\psi_\phi + R \frac{d\Omega}{dR} \hat{\xi}_R \right) \quad (7.23)$$

for $\hat{B}_R = B \partial \hat{\xi}_R / \partial z$ thus justifying Eqs. (6.12) and (6.13).

7. Derivation of the Dispersion Equation

We consider the poloidal component of the total momentum conservation equation

$$\rho \frac{\partial \hat{\mathbf{v}}}{\partial t} - \frac{1}{4\pi} (\hat{\mathbf{B}} \cdot \nabla \mathbf{B} + \mathbf{B} \cdot \nabla \hat{\mathbf{B}}) + \nabla \left(\hat{p} + \frac{\hat{\mathbf{B}} \cdot \hat{\mathbf{B}}}{4\pi} \right) + \nabla \cdot (\Delta \mathbb{P})$$

$$+ \hat{\rho} \nabla \phi_G + \rho (\hat{\mathbf{v}} \cdot \nabla \mathbf{v} + \mathbf{v} \cdot \nabla \hat{\mathbf{v}}) + \hat{\rho} (\mathbf{v} \cdot \nabla \mathbf{v}) = 0. \quad (7.1)$$

where

$$\nabla \cdot \hat{\mathbb{P}} = \hat{\mathbf{B}} \cdot \nabla [(p_{\parallel} - p) \mathbf{B}] + \mathbf{B} \cdot \nabla [(\hat{p}_{\parallel} - \hat{p}) \mathbf{B} + (p_{\parallel} - p) \hat{\mathbf{B}}]. \quad (7.2)$$

Then we apply the $\mathbf{e}_{\phi} \cdot \nabla \times$ operator on Eq. (7.1) and obtain

$$\frac{\partial}{\partial z} \left\{ \rho (\gamma_0^2 \hat{\xi}_R - 2\Omega_k \hat{v}_{\phi}) - \frac{B^2}{4\pi} (1 - \bar{p}) \frac{\partial^2}{\partial z^2} \hat{\xi}_R \right\}$$

$$- \frac{\partial}{\partial R} \left\{ \rho \gamma_0^2 \hat{\xi}_z + z \Omega_k^2 \hat{\rho} - \frac{B^2}{4\pi} \frac{\partial^2}{\partial z^2} \hat{\xi}_z + (p_{\parallel} - p) \frac{\partial^2}{\partial z^2} \hat{\xi}_z \right\} \simeq 0 \quad (7.3)$$

—

No if we consider $|1/k_R|^2 |\partial/\partial z|^2 \ll 1$ we obtain, for $|\hat{\xi}_R| > (\gamma_0/\Omega_k) |\hat{\xi}_{\phi}|$,

$$\left(\rho \Omega_D^2 \frac{\partial^2}{\partial z^2} \hat{\xi}_z \right) \frac{1}{k_R} + k_R \left\{ \gamma_0^2 \rho \hat{\xi}_z + z \Omega_k^2 \hat{\rho} + \left[(p_{\parallel} - p) - \frac{B^2}{4\pi} \right] \frac{\partial^2 \hat{\xi}_z}{\partial z^2} \right\} \simeq 0. \quad (7.5)$$

Moreover, if we refer to incompressible modes, such that $|\nabla \cdot \hat{\xi}| < \Delta_z |\hat{\xi}_z|/H_0^2$ corresponding to $\hat{\rho} \simeq -2z \hat{\xi}_z \rho_0/H_0^2$, we obtain the dispersion equation

$$\left[c_{\parallel}^2 + \frac{1}{k_R^2} \Omega_D^2 - v_A^2 \right] \frac{d^2}{dz^2} \tilde{\xi}_z - 2\Omega_k^2 \frac{z^2}{H_0^2} \tilde{\xi}_z + \gamma_0^2 \tilde{\xi}_z = 0. \quad (7.6)$$

We define

$$\bar{v}^2 \equiv c_{\parallel}^2 + \frac{\Omega_D^2}{k_R^2} - v_A^2 \quad (7.7)$$

and consider the limit where

$$\bar{v}^2 \sim \Omega_k^2 \frac{\Delta_z^4}{H_0^2} \sim \frac{p}{\rho} \frac{\Delta_z^4}{H_0^4} \quad (7.8)$$

and $\Delta_z^4 < H_0^2$. Then the solution of Eq. (7.6) is $\tilde{\xi}_z = \tilde{\xi}_{z0} \exp[-z^2/(2\Delta_z^2)]$ where

$$\frac{\bar{v}^2}{\Delta_z^4} = \frac{2\Omega_k^2}{H_0^2} \quad \text{and} \quad \frac{\bar{v}^2}{\Delta_z^2} = \gamma_0^2. \quad (7.9)$$

Consequently

$$\Delta_z = \left(\frac{1}{\sqrt{2}} H_0 \frac{\bar{v}}{\Omega_k} \right)^{1/2} < H_0 \quad (7.10)$$

for $\bar{v} < \Omega_k H_0$, and

$$\gamma_0 \simeq \left(\frac{\bar{v}}{H_0} \frac{\Omega_k}{\sqrt{2}} \right)^{1/2} < \Omega_k. \quad (7.11)$$

It is evident that the pressure anisotropy has a strong effect on the modes that can be excited. This conclusion remains valid if we consider the special case where $\hat{\rho}/\rho_0$ is given by Eq. (6.9) and D_N is positive (i.e. relatively weak temperature gradients).

9. Quadratic Form

In order to identify the factors that can contribute to the instability ($\gamma_0^2 > 0$) of the considered mode we derive a quadratic form from Eq. (8.1) by taking the integral

$$\int_{-\infty}^{+\infty} dk \tilde{\xi}_{zk}^* \left\{ \gamma_0^2 \left[1 + \frac{\kappa^2}{k_R^2} \left[1 + 4 \frac{\Omega_k^2}{\gamma_0^2 + \kappa^2 (v_A^2 - c_{\parallel}^2)} \right] \right] \tilde{\xi}_{zk} + \kappa^2 v_A^2 c_{\parallel}^2 - \frac{\Omega_D^2}{k_R^2} + \frac{\kappa^2}{k_R^2} (v_A^2 - c_{\parallel}^2) \tilde{\xi}_{zk} + \Omega_k^2 \frac{D_N}{H_0^2} \frac{d^2}{dk^2} \tilde{\xi}_{zk} \right\} = 0 \quad (9.1)$$

Considering bound solutions we have

$$\begin{aligned} & \gamma_0^2 \left\langle \left\{ 1 + \frac{\kappa^2}{k_R^2} \left[1 + \frac{4\Omega_k^2}{\gamma_0^2 + \kappa^2 (v_A^2 - c_{\parallel}^2)} \right] \right\} |\tilde{\xi}_{zk}|^2 \right\rangle \\ & \simeq \left\langle \left\{ \frac{\Omega_D^2}{k_R^2} + c_{\parallel}^2 \left(1 + \frac{\kappa^2}{k_R^2} \right) - v_A^2 \left(1 + \frac{\kappa^2}{k_R^2} \right) \right\} \kappa^2 |\tilde{\xi}_{zk}|^2 \right\rangle \\ & + \Omega_k^2 \frac{D_N}{H_0^2} \left\langle \left| \frac{d}{dk} \tilde{\xi}_{zk} \right|^2 \right\rangle \end{aligned} \quad (9.2)$$

where $\langle \rangle = \int_{-\infty}^{+\infty} dk$. Then we can see that when $c_{\parallel}^2 > v_A^2$ a new instability driving factor in addition to Ω_D^2 is introduced.

10. Quasi-Linear Momentum Flux

$$\Gamma_R^J \simeq \left\langle \left\langle \hat{u}_R (V_0 + \hat{v}_\phi^*) (n_0 + \hat{n}^*) \right\rangle \right\rangle + \text{c.c.} \quad (10.1)$$

$$= \gamma_0 \left\langle \left\langle \hat{\xi}_R \left\{ V_R + n_0 \hat{v}_\phi^* + V_0 \hat{n}^* \right\} \right\rangle \right\rangle + \text{c.c.} \quad (10.2)$$

Thus

$$R_0 \Gamma_R^J \simeq \gamma_0 n \left\langle \left\langle -2 \left(R_0^2 \frac{d\Omega_R}{dR} \right) |\hat{\xi}_R|^2 + \frac{R_0}{\Omega_0} \left[(c_{\parallel}^2 - v_A^2) \left| \frac{d\hat{\xi}_\phi}{dz} \right|^2 - \gamma_0^2 |\hat{\xi}_\phi|^2 \right] \right\rangle \right\rangle \quad (10.3)$$

and we see that $c_{\parallel}^2 > v_A^2$ a novel contribution to the flux of angular momentum has to be added to the expected quasi-linear expression for Γ_R^J .

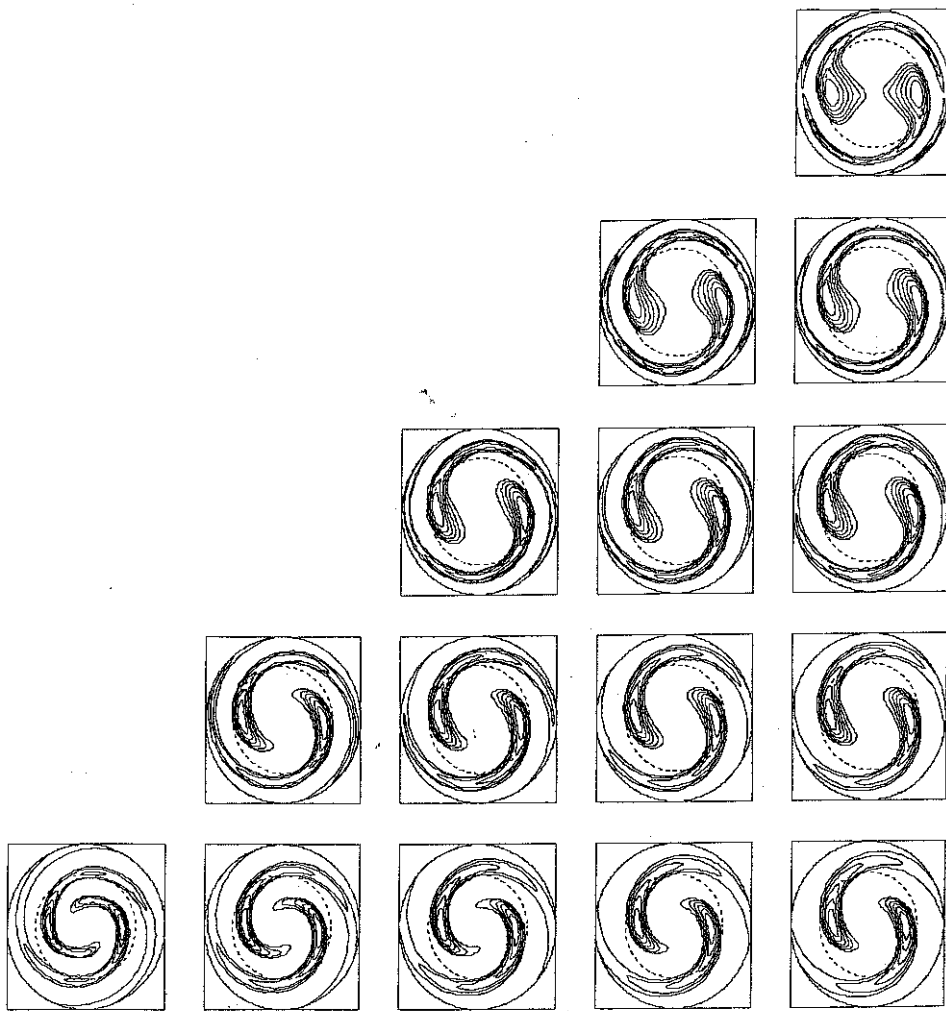


Fig. 17.2. A two-armed mode followed in a set of different models by variation of the parameters of the relevant basic state (see choice described in Section 14.4), from a wide survey of galaxy models (from Bertin, G., Lin, C.C., Lowe, S.A., Thurstans, R.P. 1989, *Astrophys. J.*, 338, 78). These are perturbed density contours (for only the positive part). The dotted circle is the corotation circle:

11. Tridimensional Solitary Ring Configurations

Tridimensional solitary ring configurations have been found to emerge, on the basis of a linearized perturbation theory, from currentless plasma disks according to the theory presented in Coppi (2009). Here we find that the presence of a temperature anisotropy can have a significant influence on the tridimensional (spiral modes) that are found following the same kind of analysis as that for axisymmetric modes described in the previous sections. Now we take $m_\phi \neq 0$ and, referring to Eq. (5.4) we consider relatively low values of m_ϕ , such that

$$\gamma_0 > m_\phi \left| \frac{d\Omega}{dR} \right| |R - R_0|. \quad (11.1)$$

Thus, defining $\gamma_T \equiv \gamma_0 + im_\phi (d\Omega/dR) (R - R_0) \equiv \gamma_0 + i\Delta\omega$,

$$\gamma_T^2 \simeq \gamma_0^2 + i2\gamma_0\Delta\omega \quad (11.2)$$

Moreover

$$\frac{\partial^2}{\partial R^2} \simeq -k_R^2 + i2k_R \frac{1}{F} \frac{dF}{dR}. \quad (11.3)$$

Then with these approximations we find

$$\tilde{\xi}_z \simeq \tilde{\xi}_{z0} \exp\left(-\frac{z^2}{2\Delta_z^2}\right) F(R - R_0) \left\{ \sin\left[k_R(R - R_0) - m_\phi(\Omega_0 t + \phi)\right] \exp(\gamma_0 t) \right\} \quad (11.4)$$

where

$$F \simeq \exp\left[-\frac{(R - R_0)^2}{2\Delta_R^2}\right]. \quad (11.5)$$

and

$$\frac{1}{\Delta_R^2} = -\frac{m_\phi}{\gamma_0} \frac{d\Omega}{dR} k_R G_0 \quad (11.6)$$

where, referring to the quadratic form Eq. (9.2),

$$G_0 \equiv \frac{\gamma_0^2 \langle |\tilde{\xi}_{zk}|^2 \rangle - \Omega_k^2 (D_N/H_0^2) \langle |d\tilde{\xi}_{zk}/dk|^2 \rangle + (v_A^2 - c_\parallel^2) \langle \kappa^2 |\tilde{\xi}_{zk}|^2 \rangle}{\gamma_0^2 \left[\langle |\tilde{\xi}_{zk}|^2 \rangle + 4 \left(\Omega^2/k_R^2 \right) (v_A^2 - c_\parallel^2) \left\langle \frac{\kappa^4 |\tilde{\xi}_{zk}|^2}{[\gamma_0^2 + \kappa^2 (v_A^2 - c_\parallel^2)]^2} \right\rangle \right]}. \quad (11.7)$$

Clearly, we require that

$$m_\phi \frac{d\Omega}{dR} k_R G_0 < 0 \quad (11.8)$$

a condition that, for $G_0 > 0$, corresponds to trailing spirals. In particular, we see that the dependence of $\tilde{\xi}_z$ on z and $R - R_0$ is very similar to that of ψ for the configurations treated as an example in Section 3.

When considering the stationary configurations that can be identified by a nonlinear analysis, we may refer again to the rings obtained in the rigid rotor limit. Then we can extend the relevant analysis by taking, for instance,

$$\mathbf{B} = \frac{1}{R} \left[\nabla \psi \times \mathbf{e}_\phi + \frac{\alpha_\phi}{\Delta_z} \psi \mathbf{e}_\phi \right] + \Delta \mathbf{B}_p \quad (11.9)$$

where

$$\psi = \psi_N \exp \left(-\frac{z^2}{2} - R_*^2 \right) \sin \left[R_* - m_\phi (\Omega_0 t - \phi) \right], \quad (11.10)$$

m_ϕ is a relatively low number, and

$$\nabla \cdot (\Delta \mathbf{B}_p) + \alpha_\phi \psi_N \frac{m_\phi}{\Delta_z R^2}$$

$$\cos \left[R_* - m_\phi (\Omega_0 t - \phi) \right] \psi_N \exp \left(-\frac{z^2}{2} - R_*^2 \right) = 0. \quad (11.11)$$

Therefore $|\Delta \mathbf{B}_p| / (|\nabla \psi|/R) \ll 1$ and, to lowest order in this ratio, the analysis given earlier should remain valid. We note, however, that $\mathbf{J} \times \mathbf{B})_\phi = \mathbf{J}_p \times \Delta \mathbf{B}_p)_\phi \neq 0$ in this case, where \mathbf{J}_p is the poloidal current. Thus as expected, a configuration represented by Eq. (11.9) involves a torque that will have to be compensated for in order to have a steady-state configuration to order $|\Delta \mathbf{B}_p|/|B_p|$.

1. Introduction

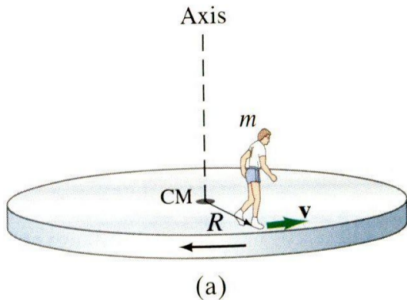
This paper is organized as follows. In Section 2, the presence of particle populations with non-thermal distributions in momentum space, in plasmas surrounding black holes, is represented dealing with plasmas having Maxwellian distributions with anisotropic temperatures in order to retain the possibility to use fluid equations. The importance of the temperature anisotropy as a sustaining factor for new axisymmetric field configurations is pointed out. In Section 3, one of the two basic non-linear equations (the Master Equation) that relate the particle density spatial distribution to the plasma pressure and to the relevant magnetic surface function, for axisymmetric stationary configurations, is derived. Moreover, the forms that the pressure anisotropy may take are discussed referring to the toroidal (azimuthal) direction or to that of the magnetic field. In this context the longitudinal pressure is taken to be larger than the transverse pressure, the latter being associated with a well thermalized particle population.

In Section 4 a new Solitary Plasma Ring configuration is identified as a significant example of those that can be found when the longitudinal pressure associated for instance with a high energy particle population, referring to the direction of the magnetic field, is prevalent and the rotation frequency is about constant over the (radial) width of the ring. The fact that the theory of these configuration does not depend on pre-existing seed magnetic field associated with currents external to these configurations is emphasized together with the fact that the magnetic field pressure is of the order of the plasma pressure. Thus the emergence of these configurations can be associated with that of magnetic fields by the combined effects of gravity and pressure anisotropy. We note that the magnetic field geometry associated with the Solitary Ring Configuration mentioned earlier involves two oppositely directed current channels.

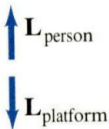
In Section 5 the importance of Magneto Gravitational Modes is discussed. These modes can be excited from a currentless standard disk with the main driving factors being the pressure anisotropy ($p_{\parallel} > p_{\perp}$) and the differential rotation within the disk. The presence of a seed magnetic field is required. These modes can be envisioned to reduce the rate of differential rotation and to produce a large amplification of the magnetic field by the currents associated with them. Thus they can be regarded as candidates for the formation of the kind of stationary configurations analyzed in Section 4. In Section 6 the analytical form of the tridimensional modes that can be excited is given. In Section 7 the linearized equations that are used in the theory of the relevant magneto gravitational modes are introduced. In Section 8 the simplest significant dispersion equation is derived showing the combination of driving factors (gravity, pressure anisotropy, differential rotation and density gradient) that the relevant modes involve. In Section 9 a more complete form of the mode dispersion equation is given and in Section 10 the associated quadratic form (in the mode amplitude) is given. This can be used to assess the mode growth rate under more general conditions than those considered in Section 8. In

Section 11 a relatively simple expression is derived for the quasi linear angular momentum transport equation connected to the theory of the considered modes.

In Section 12 the important case where magneto-gravitational modes acquire a (tri-dimensional) spiral structure with low toroidal mode numbers is treated. The characteristic density profiles are shown to be trailing spirals and the relevant modes are found to have a radially localized structure. These results anticipate, within the linear theory, the finding of a ring structure as a solution of the non-linear equations describing stationary configuration that are rigidly rotating (Section 4). In Section 13 concluding remarks on the obtained results are given. In particular, considering different factors, such as the need of giving an appropriate representation of high energy particle populations and that some of the found structures can involve relatively small characteristic distances, the importance of dealing with phase space and abandoning the limits that a fluid description of the relevant plasmas entails.



(a)



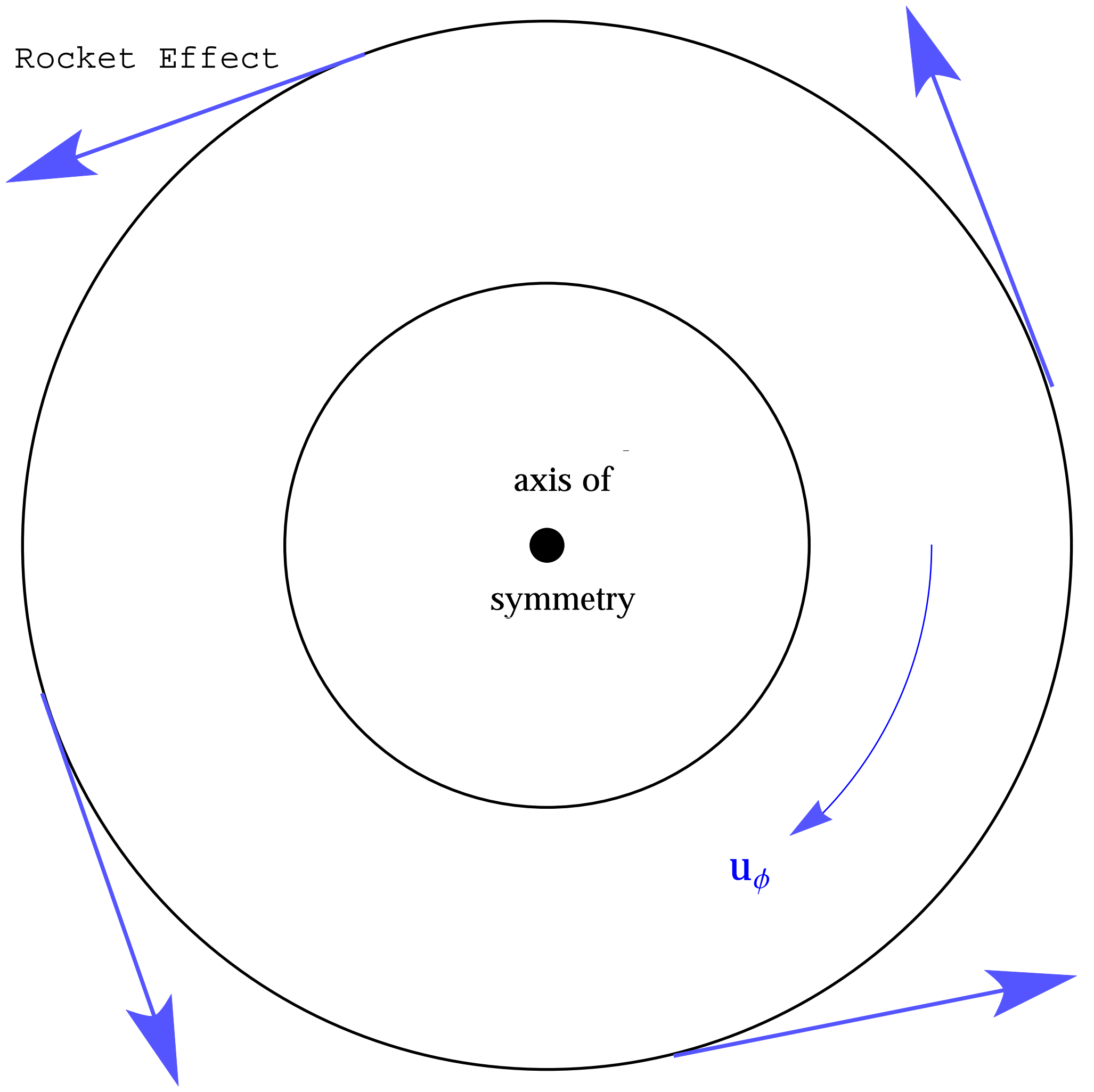
(b)

FIGURE 10–32 (a) A person standing on a circular platform, both initially at rest, begins walking along the edge at speed v . The platform, assumed to be mounted on friction-free bearings, begins rotating in the opposite direction, so that the total angular momentum remains zero, as shown in (b).

Rocket Effect

axis of
●
symmetry

u_ϕ



Locally Rigid Rotor Configurations

The Locally Rigid Rotor configurations we consider are localized over a radial scale distances $|\Delta R| < R_0$. In particular, for these configurations

$$V_\phi = \Omega_0 R \quad \text{where} \quad \Omega_0 \equiv \Omega_k (R = R_0).$$

Then

$$\Omega_0 R = \alpha_v B_\phi + \Omega(\psi) R$$

where $\nabla \cdot (\rho \mathbf{V}) = 0$ implies that $\alpha_v \rho = G(\psi)$ and

$$B_\phi = \left[\Omega_0 - \Omega(\psi) \right] \frac{R\rho}{G(\psi)}.$$

We note that in this class of configurations a seed magnetic field is not required.

Clearly, the simplest case to analyze is that with $B_\phi = 0$ and $\Omega(\psi) = \Omega_0$. Then

$$\mathbf{B} = \frac{1}{R} \nabla \psi \times e_\phi.$$